

Experimental study on the ash behaviour in combustion of pelletized residual agricultural biomass

Javier Royo^a; Paula Canalís^a; David Quintana^a; Maryori Díaz-Ramírez^b; Ana Sin; Adeline Rezeau^b

^a University of Zaragoza, c/ María de Luna 3, E-50018 Zaragoza, Spain

^b CIRCE Foundation, c/ Mariano Esquilor 15, E-50018 Zaragoza, Spain

ABSTRACT

Agricultural residual biomass presents a high potential for energy use around the world, often not utilized to a large extent due to its significant differences with respect to other biomass types, such as the one of forest origin. These differences are mainly related to the characteristics of its ashes (quantity and composition) which increase certain problematic phenomena during combustion, among them bottom ash sintering and fly ash deposition. The main goal of this paper is the experimental study of these issues for four different agropellets made of residual agricultural biomass (one woody and three blended with an herbaceous component) and a forest wood pellet (used as a reference), evaluated under different operating conditions in a laboratory fixed bed reactor. The influence of inlet air flow and temperature on the sintering degree and deposition ratio has been analyzed in a systematic way. For the five biofuels, under tested conditions, a clear relation inversely proportional between air excess ratio and deposition ratio has been determined. Deposition was more substantial for the four agropellets; meanwhile the sintering degree was more important for the three with an herbaceous component. The information obtained in this research work is intended to help researchers and technologists to make choices regarding the design and operation of conversion systems adapted for agricultural residual biomass, enhancing its market penetration.

KEY WORDS:

Biomass combustion; Agropellet; Fixed bed reactor; Ashes; Sintering; Deposition

26 1. INTRODUCTION

27 The main contribution of biomass to the renewable energy generation in the EU is found in the
28 heating and cooling sector. The 2020 target is to reach 3785 PJ in the use of biomass for heating and
29 cooling, and the contribution of solid biomass is the most important to this goal (in 2012, 2943 PJ had
30 already been achieved with this resource) [1]. Solid biomass is largely used in households for heating,
31 with an important presence of forest wood pellets. In 2012, the use of biomass in households already
32 exceeded the target set for 2020 by 10% [1].

33 In order to satisfy this growing demand, forest biomass, whose main use is still energy production, is
34 not enough [2]. The new uses foreseen in the medium term for these resources (e.g. biorefineries
35 and new materials) will hinder their increased utilization for energy production [2], [3]. For this
36 reason, it is necessary to look for new resources to satisfy the thermal energy sector. The biggest
37 increase in supply should come from the agricultural sector, where an increase of more than 150%
38 compared with 2006 is planned [1].

39 These new resources comprise mainly, apart from energy crops and some types of residual agro-
40 industrial biomass, agricultural crops residues: herbaceous crop residues and pruning residues of
41 permanent woody crops. In particular, the target of this paper are three residual agricultural
42 biomasses: vineyard pruning, corn stover and barley straw. They were selected due to their potential
43 as energy sources both in Europe and in the rest of the world. From FAOSTAT data (available at [4]),
44 it can be seen that the cultivated surface of grape, maize and barley in the EU in 2016 was 24.5 Mha.
45 Even using conservative availability indices (50% for vineyard pruning and corn stover, and 10% for
46 barley straw), their attainable residual biomass amounts to an energy potential above 500 PJ/yr.
47 Consequently, their use could contribute significantly to achieve the objectives set.

48 On the other hand, thermal conversion of agricultural biomass, mainly the herbaceous type, shows
49 clear differences with respect to that of forest origin. This is mainly due to the characteristics of the
50 ashes (quantity and composition) which give rise to certain phenomena in the conversion facility. The

51 use of a blend of woody and herbaceous biomass may reduce these problems (Zeng et al., 2016;
52 Zeng et al., 2018).

53 During combustion, ashes undergo physical and chemical transformations which cause fractioning.

54 Each of the fractions presents different problems:

- 55 • Part of the components of the ashes gives rise to a solid fraction which accumulates in the grate
56 (bottom ash, mainly constituted by e.g. calcium and potassium silicates) and can cause sintering,
57 affecting conversion in the bed, restricting the effectivity of the grate and negatively influencing
58 proper control of gaseous emissions: carbon monoxide (CO), nitrogen oxides (NO_x) and volatile
59 organic compounds (VOC) [5]-[8].
- 60 • Other part is volatilized, so when it comes into contact with zones of lower temperature, it may
61 condense in the form of small crystals (e.g., potassium chloride -KCl-, potassium sulfate -K₂SO₄-
62 and potassium carbonate -K₂CO₃-) over the surfaces of the equipment used for heat exchange. An
63 ash entrainment of solid particles in gas combustion flow from the bed to the convective areas
64 also can be produced. This phenomenon together with volatilization are responsible for
65 deposition, corrosion and erosion, which reduce performance and lifetime of the equipment.
- 66 • Additionally, some fractions of the finer particles (mostly those of size below 2.5 μm), instead of
67 leading to deposits formation, can end up being emitted as aerosols to the atmosphere, causing
68 respiratory diseases [9], [10].
- 69 • Finally, in the mass balance of the elements that constitute ashes it should be considered the
70 compounds that remain in gaseous state, such as sulfur dioxide -SO₂- or hydrogen chloride -HCl-
71 which are environmental pollutants [11]-[13].

72 During the last decades, several renowned research centers have been working towards identifying
73 key factors in biofuels conversion, as well as the transformation of their ashes, in order to predict the
74 problems generated by the latter. Although most of the published research so far concerns forest
75 biomass (e.g., [14]-[20]), there are some studies addressing agricultural biofuels (e.g., [8], [21]-[23]).

76 In all cases, it is recognized the critical influence of ash chemical composition, especially by the

77 concentration of Na, Mg, Al, Si, P, S, Cl, K and Ca [24], in the problems associated with thermal
78 conversion (e.g. sintering, deposition and emissions).

79 Notwithstanding, besides chemical composition, the ash behaviour (especially in grate boilers) is also
80 influenced by the combustion conditions in the bed, related with the design ([23]-[26]), as well as
81 with the operation mode [27].

82 In order to analyze these effects, tests can be made in commercial boilers adapted to carry them out
83 controlled [5], [8], [21], [22], [28]-[30]. However, due to the complexity of the phenomena
84 intervening in the fractioning of ashes, it is preferable to use laboratory reactors, most of them using
85 fixed bed technology, in order to have better control of combustion conditions [13], [23], [31]-[34].

86 This type of reactors makes possible to gather important information about the behaviour of fuels
87 under different operating conditions. It is possible to evaluate fuel reactivity (ignition front velocity
88 and ignition rate [35]), quantify bottom ash in the bed and determine its propensity to sintering as
89 well as quantify the amount of solid residue deposited in heat exchange surfaces (deposition ratio).
90 Furthermore, these reactors allow obtaining samples in order to characterize solid residues (bottom
91 ash and deposits), for a better understanding of the mechanisms driving ash fractioning and
92 quantifying the impact of corrosion phenomena in the heat exchange zones. In addition, carrying out
93 study of gaseous emissions (e.g. CO, NO_x or volatile organic compounds) [36]-[39], as well as those of
94 particulate material [40]-[42], is possible.

95 The main goal of this work is the analysis of the three first points (reactivity, sintering and deposition)
96 for different mixed pellets made of residual agricultural biomass (agropellets), evaluated under
97 different operating conditions in a laboratory fixed bed reactor.

98 **2. MATERIALS AND METHODS**

99 **2.1 Fuels**

100 Five different biofuels are studied in this paper. One is a forest wood pellet and four are agropellets
101 (three mixed pellets and one wood pellet):

- 102 - Forest wood pellet:
- 103 • Pine pellet (PP) -pellet A1, according to ISO 17225-2-: it will be used as a reference to
- 104 record the differences from fuels of residual agricultural origin.
- 105 - Agricultural residual pellets (agropellets):
- 106 • Wood agropellet: 100% Vineyard pruning pellet (PV)
- 107 • Mixed pellet (with an herbaceous component):
- 108 ○ 70% Vineyard pruning + 30% Barley straw (PVB)
- 109 ○ 70% Vineyard pruning + 30% Corn stover (PVC)
- 110 ○ 60% Vineyard pruning + 20% Corn stover + 20% Barley straw (PVCB).

111 Tables 1 and 2 show the main thermochemical properties of the selected fuels.

112 Table 1. Fuels properties

		PP	PV	PVB	PVC	PVCB
Bulk density (kg·m⁻³)¹		674	599	562	556	546
Proximate analysis (% m/m d.b.)	Volatile matter ²	84.2	76.5	72.4	72.1	72.3
	Fixed carbon ⁸	15.4	20.5	21.7	18.6	21.2
	Ash ³	0.4	3.1	5.9	9.3	6.5
Total Moisture (% m/m w.b.)⁴		7.2	9.0	9.1	9.2	9.0
Ultimate analysis (% m/m d.b.)	Carbon ⁵	50.9	48.9	46.36	46.01	46.36
	Hydrogen ⁵	6.1	5.8	5.77	5.64	5.55
	Nitrogen ⁵	0.09	0.55	0.56	0.55	0.60
	Sulfur ⁶	< 0.01	0.09	0.055	0.050	0.094
	Chlorine ⁶	0.01	0.03	0.047	0.080	0.090
	Oxygen ⁸	42.49	41.6	41.29	38.33	40.58
HHV (d.b. at p=constant) (MJ·kg⁻¹)⁷		20.43	19.11	18.54	18.06	18.36
LHV (w.b. at p=constant) (MJ·kg⁻¹)⁷		17.55	16.01	15.48	15.06	15.40

113 ¹ EN 15103:2009 ² EN-ISO 18123:2016 ³ EN-ISO 18122:2016 ⁴ EN-ISO 18134:2016 ⁵ EN-ISO 16948:2015

114 ⁶ EN-ISO 16994:2015 ⁷ EN-ISO 14918:2011 ⁸ Calculated

115

116

117

118

119

120

121 Table 2. Ashes properties

		PP	PV	PVB	PVC	PVCB
Chemical ash composition (% m/m d.b.)⁹	Al ₂ O ₃	2.1	0.91	2.72	2.19	2.30
	CaO	24	42.39	45.77	48.17	40.54
	Fe ₂ O ₃	1.8	0.71	2.22	1.98	1.27
	K ₂ O	13	30.09	14.88	15.79	19.43
	MgO	9.9	10.45	8.64	7.64	11.01
	Na ₂ O	1.8	0.62	0.41	0.39	0.38
	P ₂ O ₅	8.5	7.35	4.45	4.00	4.36
	SO ₃	4.4	3.95	2.32	3.24	4.39
	SiO ₂	15	2.65	17.70	15.31	15.22
	TiO ₂	0.078	0.07	0.17	0.18	0.16
	Cl	-	0.12	0.21	0.57	0.54
Ash melting temperatures oxidant conditions (°C)¹⁰	Initial deformation temperature (DT)	> 1400	1240	1130	1310	1330
	Hemisphere temperature (HT)	> 1400	> 1500	1310	1460	1460
	Flow temperature (FT)	> 1400	> 1500	1370	1480	1470

122 ⁹ EN-ISO 16967:2015 ¹⁰ CEN/TS 15370-1:2006

123 2.2 Reactor

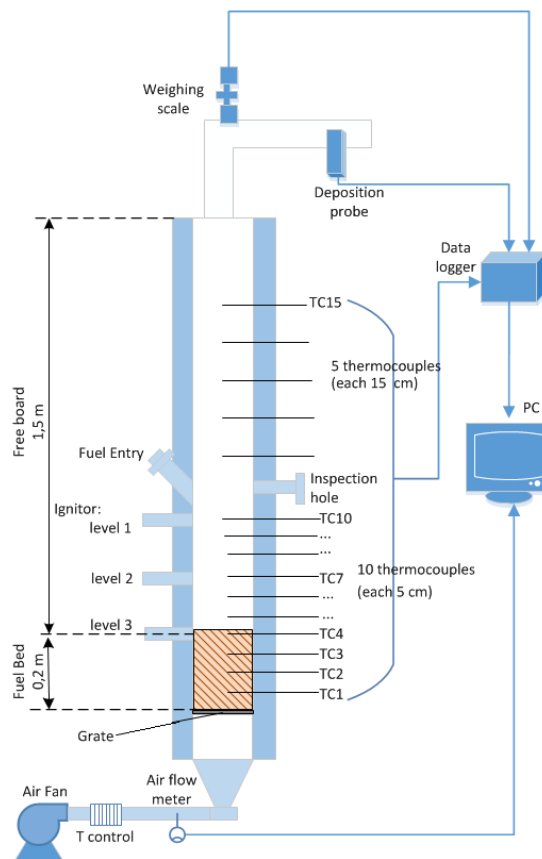
124 As previously mentioned, it is very difficult to obtain accurate data using commercial equipment,
 125 even a modified one. Thus, for research purposes, it is usual to resort to laboratory reactors. In the
 126 case of fixed bed reactors simplified geometries are usually used, such that the behaviour is
 127 considered one-dimensional [43].

128 The main variable in fixed bed commercial equipment is space, since by different means, biomass
 129 moves through the grate while experiences several processes: heating and drying of the fuel,
 130 volatiles release, and, finally, combustion of the char. However, in laboratory reactors, fuel
 131 undergoes these processes successively [35]. Fuel is fed in batches, i.e., certain amount is introduced
 132 in the reactor and after combustion, ashes are removed, to be added a new load of fuel. This
 133 operation mode greatly simplifies design, facilitates data acquisition and allows better control of the
 134 reactor.

135 In order to perform the tests, an experimental fixed bed reactor has been adapted (see Fig. 1). It was
 136 designed and set up by CIRCE for a previous project [44]. It consists of a vertical cylindrical combustor
 137 chamber made of stainless steel AISI-310S, with a height of 1700 mm and an inner diameter of 200

138 mm. There is an insulating material between the external side and the combustor chamber. At the
139 bottom, there is a grate with 3 mm diameter holes separated equidistantly resulting in a porosity of
140 4.5%.

141 Combustion air is injected from the bottom, through the orifices in the grate, by means of a fan
142 equipped with a variable-frequency drive that allows adjusting the air flow. Since tests are carried
143 out at a controlled temperature of the combustion air, it is arranged to use a refrigerator or an
144 electrical resistor at the inlet air, to cool down or heat up (see Fig. 1). Besides, a hot wire flow meter
145 is located after the fan to measure the temperature and the velocity of the introduced air.



146
147 Fig. 1. Scheme of the experimental test facility

148 Combustion inside the reactor can be regarded as counter current, given the relative movement of
149 the air flow and the ignition front. While the latter moves from the upper part of the reactor towards
150 the base, the combustion air, as is already indicated, is injected from the grate located in the lower
151 part of the reactor. In this configuration, radiation and conduction drive the ignition front in the
152 opposite direction to the flow of combustion air. The latter, through convection, retains to some

153 extent the advance of the ignition front [43]. Combustion gas exits through a pipe located near the
154 top.

155 Fifteen N-type thermocouples are inserted along the chamber wall. They perform the measurement
156 in the center of the combustion chamber and, as can be seen in Fig. 1, they are aligned. For
157 identification purposes, they are numbered from TC1, the closest to the grate, to TC15, located in the
158 upper part of the reactor. The first ten are located 5 cm from each other (from TC1 to TC10), and the
159 other five each 15 cm apart. The reactor is suspended from a weighting scale that allows monitoring
160 the mass loss of the fuel bed.

161 In addition, the facility has been completed by installing a deposition probe with a removable
162 sampling ring in the chimney of the reactor (see Fig. 1) [45]. This is a common device used to
163 simulate the deposition of ashes in furnace pipes and heat exchangers [46]. The sampling ring used
164 to extract samples of the deposits is cooled by compressed air, allowing to keep its surface at an
165 appropriate temperature for studying deposition [45]

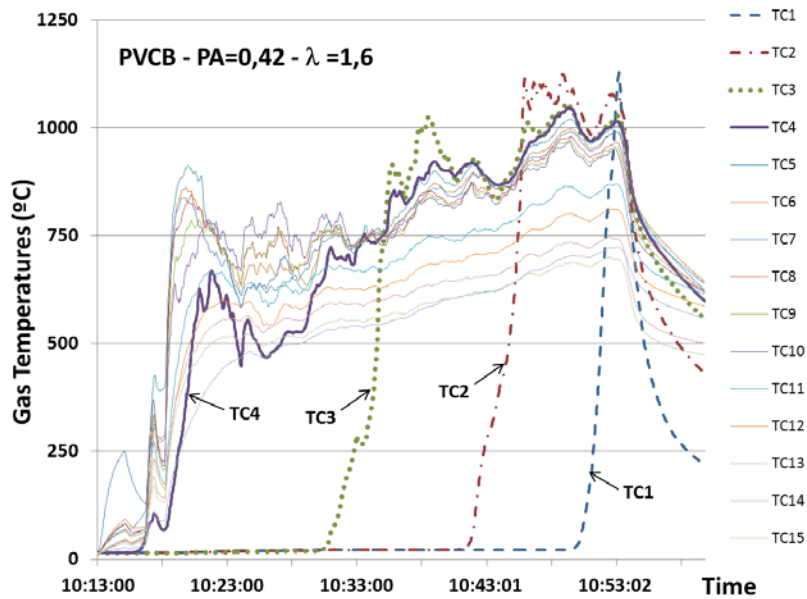
166 **2.3 Test protocol**

167 In this section the relevant features of the tests performed with the laboratory reactor are
168 presented. A total of 82 tests have been carried out with the five fuels following the same protocol.
169 All of them were carried out with an excess air ratio in the range from 1 to 2.3 (over-stoichiometric
170 conditions), in order to reproduce the combustion conditions found in small, domestic equipment.

171 The parameters that have been varied in the tests, besides the fuel type, are:

- 172 • Inlet air flow ($PA, kg \cdot m^{-2} \cdot s^{-1}$), expressed as the air mass flow by unit area of the grate
- 173 • Inlet air temperature ($Ta, ^\circ C$). According to this parameter, there are two types of test for
174 each fuel: without pre-heating (inlet air at 25 °C), and with pre-heating (inlet air at 80 °C).

175 The amount of biomass fed to the reactor in each test is such that the total bed height is 210 mm. In
176 this way, thermocouples TC1 to TC4 are initially set inside the bed. Fig. 2 shows the evolution of the
177 temperatures registered by the 15 thermocouples inside the reactor during one of the tests.

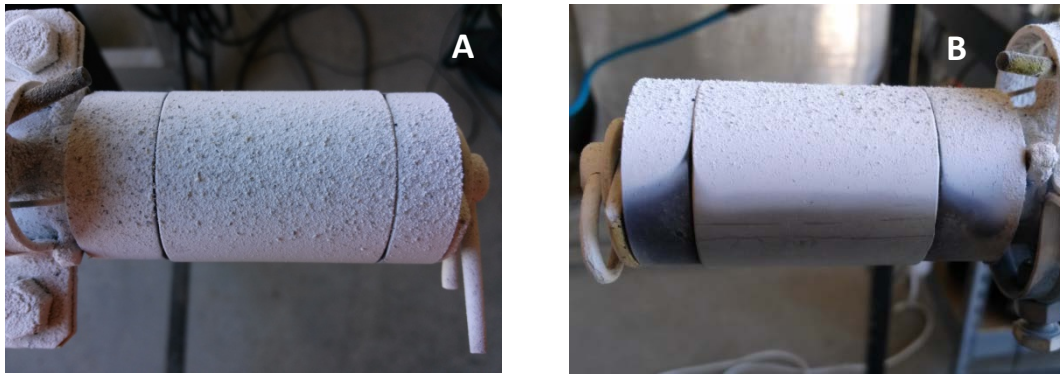


178

179 Fig. 2. Temperature profiles. Reactor test with PVCB – PA=0.42 kg·m⁻²·s⁻² – Ta=25 °C - λ=1.6.

180 The reaction is triggered by an ignitor placed above the fuel bed, which causes the temperatures of
 181 the biomass to increase (upper thermocouples). Once combustion is initiated, and biomass is being
 182 consumed, the temperature registered by thermocouples placed along the fuel bed rises, from TC4
 183 to TC1 (Fig. 2). They represent the increase of the fuel temperature as the ignition front propagates.
 184 Once all the fuel has been consumed, temperatures start to decrease. It is considered as stable
 185 combustion period, to perform calculations, the time lapsed from TC3 reaching 500 °C, so the fuel
 186 above TC3 has been consumed and there has been enough time for the combustion to stabilize, until
 187 TC1 reaches the same reference temperature, and the only remaining fuel is that between this
 188 thermocouple and the grate.

189 During the stable combustion period, the deposition probe is inserted inside the chimney. The
 190 removable sampling ring has been previously cleaned, dried and weighed. The compressed air for
 191 refrigeration is adjusted so that the average temperature of the sampling ring is 335±25 °C. Once
 192 extracted (see Fig. 3) the dirty sampling ring is dried and weighed again to obtain the amount of mass
 193 deposited. Using this weight value and the surface of the sampling ring it is possible to calculate the
 194 deposition rate [REFERENCIAS], allowing to estimate the tendency to fouling of each studied fuel.



195

196 Fig. 3. Removable sampling ring. Reactor test with PVB – $PA=0,40 \text{ kg}\cdot\text{m}^{-2}\cdot\text{s}^{-2}$ – $T_a=25^\circ\text{C}$ – $\lambda=1.37$ – $DR = 26.1$
 197 $\text{g}\cdot\text{m}^{-2}\cdot\text{h}^{-1}$ – A: Frontal view, B: Lateral view.

198 Besides the aforementioned variables, once combustion is complete and the reactor has cooled down,
 199 bottom ashes are collected from the top of the grate for weighing and classification (see Fig. 4). The
 200 determination of sintering degree with the sieving and weighting bottom ash fractions has been used in
 201 several studies to determine the slag tendency of a fuel ([5], [47], [48]). In this case, the
 202 following categories, based on a revised classification of sintering degree defined in a previous work
 203 [21], are used: S1, pass through a 3.15 mm sieve and are considered as not sintered; S2, do not pass
 204 the 3.15 mm sieve, but are easily disaggregated by hand and present a low degree of sintering; S3, do
 205 not pass the 3.15 mm sieve, are difficult to disaggregate by hand and present a high degree of sintering.
 206 Since the difference between S2 and S3 is subjective, a fraction S2/3 encompassing both classes is used.



207

208 Fig. 4. Bottom ashes. Reactor test with PVC – $PA=0.41 \text{ kg}\cdot\text{m}^{-2}\cdot\text{s}^{-1}$ – Inlet $T_a=25^\circ\text{C}$ – $\lambda = 1.27$

209 From the inlet parameters (PA y T_a), the measured variables, the geometrical data and the fuel
 210 analysis, the following parameters are calculated:

- 211 ○ **Air velocity in the grate (V_{PA} , $m \cdot s^{-1}$):** it is quantified from the mass flowrate of combustion air
212 injected during the test (PA), its inlet temperature (T_a), and the inlet area (grate hole).
- 213 ○ **Velocity of the ignition front (v_{ir} , $m \cdot s^{-1}$):** it is a measure of how fast the flame progresses along
214 the fuel bed height. It is calculated from the time that takes for consecutive thermocouples
215 (TC3, TC2 and TC1) to reach a pre-determined temperature (reference value 500 °C) and the
216 known distance between them (50 mm).
- 217 ○ **Ignition rate (m_{ir} , $kg \cdot m^{-2} \cdot s^{-1}$):** it is obtained by multiplying the velocity of the ignition front (v_{ir}) by
218 the bulk density of the fuel, which allows comparing the combustion behaviour of different fuels
219 [43]. It is expressed as mass loss per grate surface area (ignition front plane area) and time.
- 220 ○ **Excess air ratio (λ):** once the ignition rate (m_{ir}) has been determined, the excess air ratio for
221 each test can be calculated from the mass flowrate of combustion air injected during the test
222 (PA), and the stoichiometric air-to-fuel ratio of the studied fuel.
- 223 ○ **Mean flame temperature (TC3m, °C):** average value of the temperature registered by TC3
224 between the instant when TC2 and TC1 reach 500 °C.
- 225 ○ **Deposition rate (DR, $g \cdot m^{-2} \cdot h^{-1}$):** it is obtained from the mass of ash deposits collected, the area
226 of the ring surface and the duration of the exposition.

227 3. RESULTS AND DISCUSSION

228 Table 3 summarizes the main features of the tests performed. In the following section, the main
229 characteristics and combustion behaviour differences among the fuels observed during the tests are
230 presented regarding the different combustion parameters, the bottom ash and ash deposits
231 collected by the probe.

232

233

234

235

236

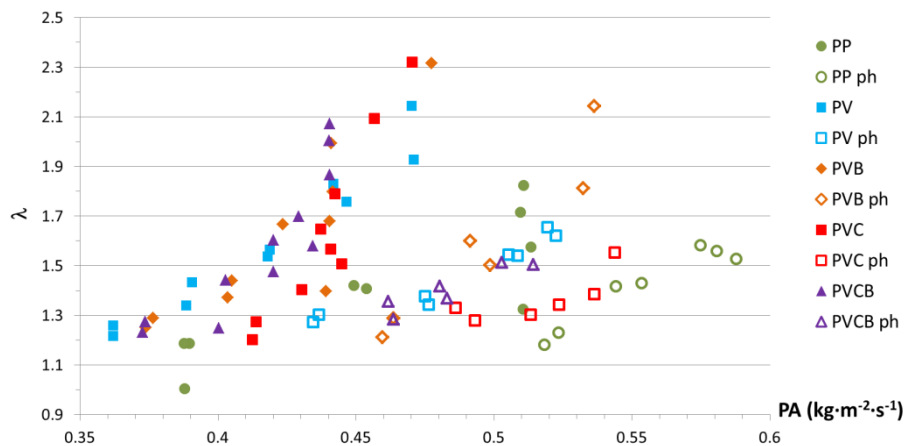
237 Table 3. Summary of test features

		PP	PV	PVB	PVC	PVCB
Number of tests performed	Without pre-heating (Ta=25 C°)	9	10	10	9	11
	Pre-heated test (Ta=80 C°)	7	8	6	6	6
PA (kg·m ⁻² ·s ⁻¹)	Min	0.39	0.36	0.37	0.41	0.37
	Max	0.59	0.52	0.54	0.54	0.51
λ	Min	1.00	1.15	1.21	1.18	1.23
	Max	1.95	2.04	2.30	2.29	2.07
Fed fuel (kg)		4.40	4.03	3.78	3.74	3.67

238

239 3.1. Combustion parameters

240 One of the fundamental parameters used to characterize combustion is λ . In Fig. 5, this parameter is
 241 shown as a function of PA for all tests, including those in which Ta was 25°C, and those in which this
 242 value was set at 80°C (pre-heated test, namely, ph).

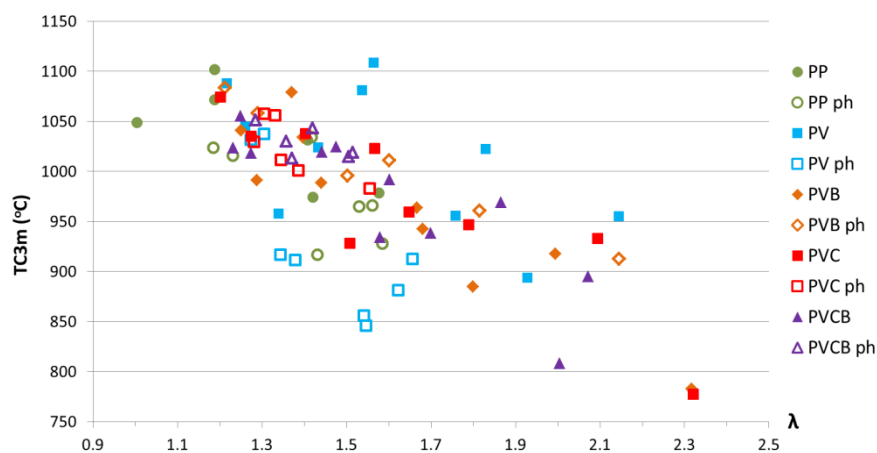


243

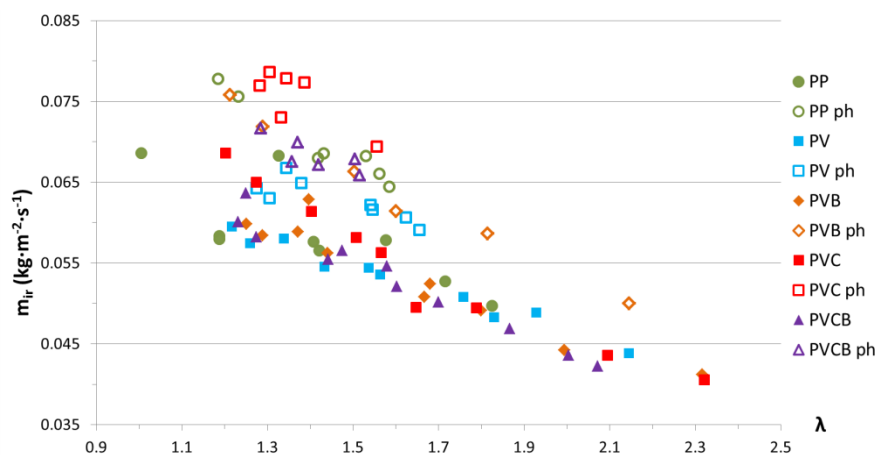
244 Fig. 5. Relation between excess air ratio (λ), inlet air flow (PA) and inlet air temperature (Ta).

245 As could be expected, for each fuel, given Ta (25°C or 80°C), λ increased with PA. PA supplied and,
 246 therefore, λ is the key parameter influencing the behaviour of the ignition front. Previous studies
 247 involving fixed bed reactors in literature have shown that, depending on PA supplied, different
 248 combustion regimens might appear [43], [49], [50]. There is a first regime, generally corresponding to
 249 λ values lower than 1 (sub-stoichiometric conditions), where the deficient amount of oxygen is the
 250 limiting parameter for combustion. In this case, an increase in PA supplied accelerates the
 251 propagation of the combustion front (higher m_{ir}) and causes that the reaction temperatures raise. If

252 PA supplied is increased further, generally corresponding to λ values higher than 1 (over-
 253 stoichiometric conditions), the behaviour is different. In this regime, as the air supplied increases, the
 254 fuel bed temperatures decrease and the flame propagation process slows down (lower m_{ir}) [43], due
 255 to the convective cooling. This general tendency is depicted for all the tested fuels in Fig. 6 and Fig. 7,
 256 where as λ values increase (higher than 1 in all the cases), m_{ir} and TC3m gradually decrease. This
 257 decrease in m_{ir} values means that the relation between λ and PA shown in Fig. 5 (for a constant T_a) is
 258 not exactly lineal.



259
 260 Fig. 6. Mean flame temperature (TC3m) versus excess air ratio (λ) for all fuels



261
 262 Fig. 7. Ignition rate (m_{ir}) versus excess air ratio (λ) for all fuels

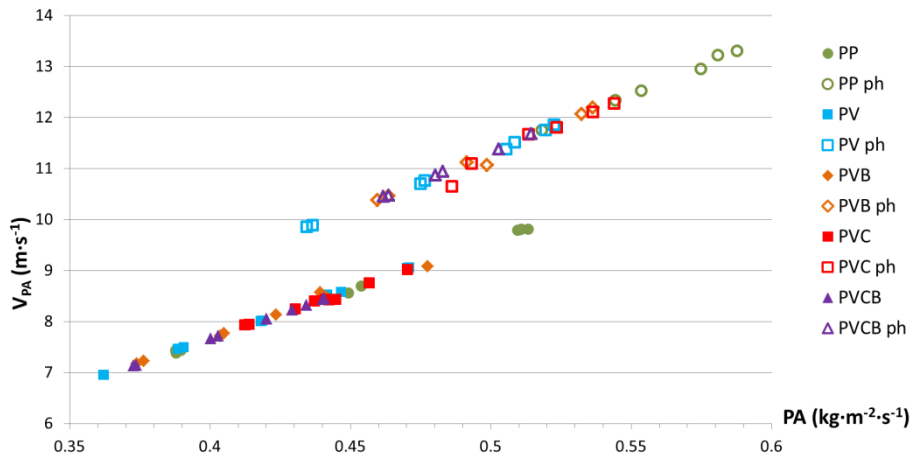
263 In any case, given the interdependency for each fuel between m_{ir} , λ and TC3m, for purposes of
 264 clarity, in some of the following discussions it will be more interesting to use λ instead of PA as the
 265 parameter related to the amount of combustion air.

266 Regarding the influence of T_a , it can be seen in Fig. 5 that in order to attain a certain λ it is necessary
267 to work with higher PA in the case of pre-heated air. This is because pre-heating primary air causes
268 an increase in m_{ir} for all fuels and conditions tested, as can be seen in Fig. 7, due to a higher T_a does
269 not lead to such a pronounced convective cooling, while it improves drying and ignition. The increase
270 in m_{ir} achieved by pre-heating the inlet air is around 15-20% for the different fuels. However, the
271 combustion temperatures in the bed (represented by TC3m) are not clearly influenced by T_a , except
272 in the case of PV (see Fig. 6).

273 Concerning the comparison of the values of TC3m and m_{ir} among the tested fuels, there are not
274 significant differences. All fuels reach similar TC3m values, except PV which shows a great variability.
275 There is a wide variety of properties that influence the behaviour of a fuel during combustion, some
276 are related to its composition (elemental composition, ash content, moisture, heating value or
277 volatiles and fixed carbon ratio) and some are related to its physical characteristics (particle size and
278 shape, particle durability or bed porosity). Previous studies in literature have tried to relate the
279 behaviour of the propagation front with some characteristics of the fuel [41], [43], [49], [51]-[53]. As
280 all the fuels tested in this paper are pelletized and present similar moisture values, no remarkable
281 differences were expected in the m_{ir} and TC3m values and behaviour. It is very difficult to draw
282 conclusions on the slight differences and tendencies observed as all the characteristics influence the
283 parameters under study in a different and interrelated manner.

284 It has been also observed that for all test, PA and, therefore, V_{pa} , not only affects the combustion
285 behaviour but also ash entrainment. In Fig. 8 the relationship between these two variables is
286 depicted. As it was expected, the relationship between PA and V_{pa} is linear and clearly affected by the
287 presence of pre-heating, due to this velocity is proportional to T_a . To attain similar λ values during tests
288 with and without pre-heating, greater PA values were needed for the tests with higher T_a and,
289 accordingly, higher values of V_{PA} are obtained in these cases.

290

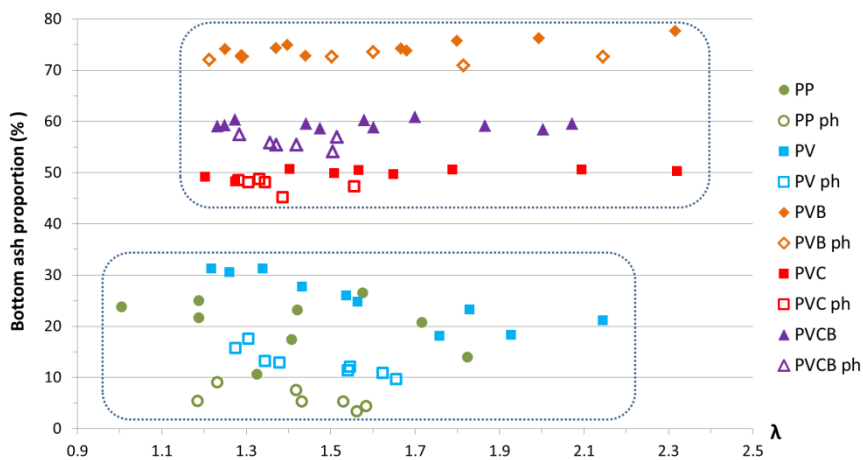


291
292 Fig. 8. Air velocity in the grate (V_{PA}) versus inlet air flow (PA) for all fuels.

293 **3.2. Bottom ash**

294 In terms of the bottom ash fraction and its sintering degree, important findings have been elucidated
295 for all the tested fuels.

296 As it is depicted in Fig. 9, considering each fuel separately it can be noticed that the largest bottom
297 ash proportion (% obtained with respect to the total amount of ash introduced with the fuel) is
298 around 75% and corresponded to PVB, followed by PVCB and PVC pellets, with 60% and 50%
299 respectively. On the contrary, the lowest proportion of gathered bottom ash (around 5-30%) is
300 reached by PP and PV, in that order. Considering these results, it seems that tested pellets can be
301 divided into two main groups: the first one is formed by wood pellets (PP and PV) whereas the
302 second group corresponds to mixed pellets (PVB, PVC and PVCB).



303
304 Fig. 9. Bottom ash proportion (% with respect the total amount of ash introduced with the fuel) versus excess
305 air ratio (λ) for all fuels.

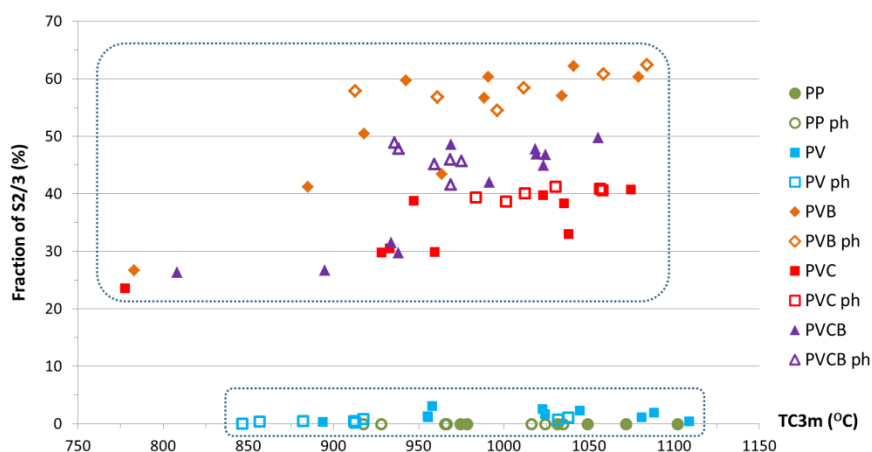
306 For the mixed pellets the proportion of bottom ash gathered is generally unaffected by λ . This trend
 307 could suggest that for all combustion temperatures (from 775°C) the expected ash fractioning is
 308 reached, leading to the remaining bottom ash fraction on the grate whereas the more volatilized
 309 components are released and carried out with the gases. However, it could also mean a decrease of
 310 the quantity of volatilized ash, due to the lower combustion temperature, compensated with the
 311 expected increase of ash entrainment, due to the larger air velocity.

312 With regard to woody fuels, both the low quantity of bottom ash, and its reduction upon increasing
 313 λ , could be related to a high degree of particles entrainment.

314 Also, it is important to mention that almost all the fuels show a lower percentage of bottom ash for
 315 tests with pre-heated air. These tests were carried out with a higher air velocity and a slightly higher
 316 combustion temperature, and consequently a larger ash entrainment and vaporization, respectively,
 317 could be expected. Nevertheless, this fact is much less clear in PVB case and much more in PV case.

318 The sintering degree of bottom ash is key to analyze the behaviour of the fuel, due to the problems
 319 that these structures can generate during the development of combustion and for the equipment.

320 In Fig. 10 it is shown the ash fraction S2/3 found in the bottom ash (as a percentage respect to the
 321 total amount of ash introduced) as a function of TC3m (with- and without pre-heating).



322
 323 Fig. 10. Fraction S2/3 of the bottom ashes (% with respect the total amount of ash introduced with the fuel)
 324 versus the mean flame temperature (TC3m) for all fuels.

325 Again the two groups of fuels show different behaviour: while wood pellets present low quantities of
 326 S2/3 fraction (below 3% for PV and negligible for PP), in line with the high values of HT and FT

327 presented by these fuels (Table 2), for mixed pellets the percentages are much higher (between 24
 328 and 63%). Among the mixed pellet, PVB stands out due its high sintering degree, which is also in line
 329 with its lower ash melting temperatures (Table 2).

330 From Fig. 9 and Fig. 10 is clear the relationship between the sintering degree and the percentage of
 331 retained ash, since the fuels with greater sintering degree show a greater amount of bottom ash as
 332 well. This could be because a high degree of sintering precludes particles entrainment.

333 In Fig. 10 can also be observed the clear increment of the sintering degree upon increasing TC3m, at
 334 least until 900-1000°C depending on the fuel, from that point values are almost constant.

335 Concerning the effect of preheated air, it can be seen from Fig. 10 that not significant differences
 336 have been generally detected for the S2/S3 proportion.

337 It is difficult to completely explain the differences in the behaviour of fuels, especially in the case
 338 between the PV and the rest of residual agricultural pellets, relying only in the chemical composition
 339 of the ashes shown in Table 2., because the phenomenon of sintering and slagging depends not only
 340 on chemical composition but also on its mineral origin [54]. Nevertheless, some important
 341 characteristics can be analyzed considering molar ratios presented in Table 4., based on earlier
 342 research studies [22].

343 Table 4. Molar ratios

Ratio label	Ratios	PV	PVB	PVC	PVCB
I	Si/P	0.43	4.70	4.52	4.12
II	(K+Na+Ca+Mg)/(Si+P)	11.34	3.81	4.49	4.51
III	(Ca+Mg)/(K+Na)	1.54	3.13	3.01	2.35

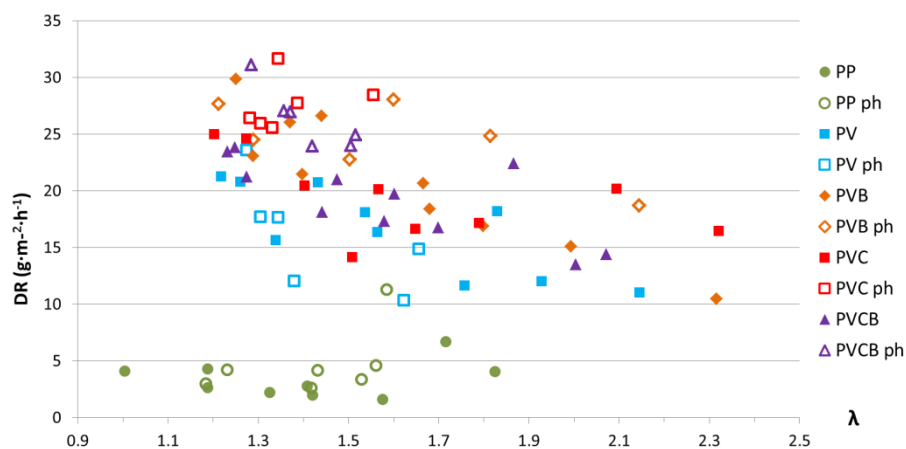
344
 345 Considering molar ratio I, Si/P, it is evident that bottom ash is Si-dominated for all mixed pellets (PVB,
 346 PVC and PVBC). For PV, besides Si-compounds expected to be retained in bottom ash, P interactions
 347 might result into a P-compounds distribution among bottom and fly ashes. Furthermore, comparison
 348 of molar ratio II suggests that there is a surplus of alkali components compared to (Si+P) for all the
 349 four agricultural fuels. According to molar ratio III, this surplus is formed by a larger fraction of
 350 alkaline earth elements (Ca+Mg) than the one for the alkali metals (K+Na).

351 It is generally expected that presence of alkaline earth oxides will rise the melting temperatures of
 352 alkali silicates, which largely will contribute to overcome occurrence of severe sintering. The excess
 353 of alkaline earth elements will remain in the residual ash limiting the sintering tendency whereas the
 354 alkali metal fraction will be volatilized and, consequently, will contribute to the formation of fine
 355 particulate emissions and deposits. Nevertheless, this beneficial effect to limit sintering behaviour is
 356 surely minimized for the mixed pellets due to the surplus of Si (see ratio I). Consequently, silicates of
 357 lower melting temperature (K/Ca/Silicates) are formed contributing to the achieved sintered ashes.
 358 This was not the case of PV, due to its low value of molar ratio I.

359 3.3. Deposition

360 Deposits were settled chiefly on the upstream side of the probe, with only a very marginal portion
 361 downstream (see Fig. 3), similarly to other results found in literature [35], [54].

362 In Fig. 11 it is shown DR as a function of λ (with- and without pre-heating).



363
 364 Fig. 11. Deposition ratio (DR) versus excess air ratio (λ) for all fuels.

365 As expected, DR for PP is very small (around $5 \text{ g}\cdot\text{m}^{-2}\cdot\text{h}^{-1}$), mostly due to the reduced amount of ash
 366 this fuel shows (lower than 1 wt-% d.b.). This fact, positive regarding ash behaviour, makes it difficult
 367 to find trends for this fuel.

368 For agropellets, the worst conditions are attained for the lower values of λ (around 1.2)
 369 corresponding to DR in the range of $20\text{-}32 \text{ g}\cdot\text{m}^{-2}\cdot\text{h}^{-1}$. Although it is difficult to compare these ratios
 370 with those obtained in other tests found in the literature due to differences in conversion

371 technology, fuel composition, placement of the probe, surface temperature, etc., it can be suggested
372 that these values are of the same order of magnitude of those obtained in the experiments and
373 simulations gathered for similar fuels and combustion conditions [56].

374 Despite no significant differences are identified among agropellets, based on the quantitative results
375 comparison of their deposition tendency might be according to the following order:
376 PVC>PVCB>PVB>PV. This suggests that the fuels with an herbaceous component are the more
377 troublesome ones.

378 It may be surprising the lower DR of PV compared to the rest of agricultural fuels, given the high
379 concentration of K in its ash (i.e., 30.09 wt-% d.b. expressed as K_2O , compared to 14.88 wt-% d.b. %-
380 20.54 wt-% d.b. % for the others), and considering that K is one of the elements that might
381 contribute to a greater tendency of fouling [57]-[59]. However, it is necessary to take into account
382 that the percentage of ash for PV is much lower than for mixed pellets (3.1 wt-% d.b. % compared to
383 5.9 wt-% d.b. %- 9.3 wt-% d.b.%), which implies that the amount of K per fuel unit mass is
384 significantly lower. In addition, it should be considered its very different content of Cl and S in PV
385 compared to the mixed pellets (see Table 2):

- 386 • The content of Cl is lower in the case of PV, which does not facilitate the transfer of K in the
387 flue gas [57], [60], [61].
- 388 • The content of S is relatively high, which implies a low value for the Cl/S molar ratio in the
389 feed ash that might facilitates formation of K-sulphates. These compounds can be retained in
390 the bottom ash fraction in the temperature range of 850–1000°C [23].

391 For all the agropellets it is clearly observed that upon increasing λ there is less deposition in the
392 probe. To analyze this result is necessary to take into account that the ash transformation reactions
393 may be influenced by a lot of factors: temperature, residence time, air supply, flue gas velocity, etc.
394 [24]. In spite of the complexity of the deposition process, it can be stated that, as observed in section
395 3.2, a larger flow of combustion air might contribute to a larger ash entrainment, which in certain
396 circumstances (particles composition, velocity and temperature of the gas, temperature of the

397 surfaces, etc.) can be deposited on the exchange surfaces, increasing deposition. Likewise, this
398 increase in the air flow causes a reduction of the mean flame temperature, which may limit the
399 volatility degree of main reactive ash elements that participate on the deposition mechanisms (e.g.,
400 K, Cl, S) and consequently, a lower DR can be obtained [64], [65]. Hence, the reduction of DR upon
401 increasing λ suggests that volatilization of reactive elements was the dominant effect in the
402 deposition phenomenon, compared to a possible contribution of the entrained of ash.

403 It is worth noting that for mixed pellets it is perceptible a slightly increase in DR when using pre-
404 heating. This may be mostly due to an increase in the particles entrainment since, as already
405 discussed, the pre-heated tests were carried out with higher PA, which causes a higher speed in the
406 bed without significantly increasing TC3m. This rise in DR with pre-heating can be quantified (for the
407 same λ) in approximately a 10% for PVB, a 20% for PVCB and 30% for PVC. The amount in which
408 different herbaceous fuels are affected is clearly related to the sintering tendencies (see Fig. 10 and
409 Fig. 11), reflecting the fact that a higher sintering degree tendency implies a lower amount of ash
410 available to be dragged, in spite of an increase in the air velocity.

411 Notwithstanding, in the case of PV it is not observed an increase of DR in the tests with preheating,
412 which is apparently at odds with the noticeable increase of particle entrainment with pre-heating, as
413 shown in Fig. 11. In other words, pre-heating produces, for PV, a rise in ash entrainment but not in
414 deposition. Although it is necessary to study this effect more carefully, it could be related to a great
415 predominance for this fuel of the mechanism of condensation (condensed deposits) in the deposition
416 against the inertial impact.

417 In any case, both in the case of sintering (section 3.2) and in the case of deposition (section 3.3), the
418 complexity of the combustion processes makes it difficult to draw clearer conclusions as it is also
419 mentioned in [25]. Nevertheless, additional information to support these trends will be obtained
420 from the ash characterization to be carried out by SEM-EDS and P-XRD as the continuation of this
421 research study.

422

423 4. CONCLUSIONS

424 This study provides systematical experimental results on five biomass pellets combustion in a
425 laboratory fixed bed reactor, regarding the influence of inlet air flow and temperature on
426 combustion parameters, bottom ash characteristics, and ash deposition.

427 The work carried out has confirmed that for all fuels analyzed, as the excess air ratio increases
428 (higher than 1 in all the cases) the velocity of the ignition front (and therefore the ignition rate) and
429 the combustion temperature gradually decrease. Also it has been observed that the influence of the
430 inlet air temperature is greater on the ignition rate than on the combustion temperature.

431 Important differences in the quantity and sintering degree of bottom ash among the five fuels have
432 been observed. Tested pellets can be divided into two main groups: the first one is formed by wood
433 pellets (PP and PV) with low bottom ash proportion and low quantity of S2/3 fraction (around 5-30%
434 and 0-3%, respectively, with respect to the total amount of ash introduced with the fuel), whereas
435 the second group corresponds to mixed pellets (PVB, PVC and PVCB) with much higher values of
436 these parameters (around 50-75% and 24-63%, respectively).

437 Concerning deposition, a clear relation inversely proportional between air excess ratio and
438 deposition ratio has been determined for the four agropellets (PV, PVB, PVC and PVCB). Thus, the
439 worst conditions were attained for the lower values of λ (around 1.2) corresponding to deposition
440 ratios in the range of 20-32 g·m⁻²·h⁻¹.

441 The data provided in this paper is intended to complement the existing knowledge of the influence of
442 excess air ratio on efficiency and emissions (mainly CO and NO_x), in order to support the decision
443 making process concerning the design and operation of conversion systems suitable for agropellets.

444 Only a preliminary evaluation of the mechanism involved into the sintering and deposition
445 phenomena and their relation with fuel composition has been carry out. In order to gain a better
446 understanding on these issues, additional information will be obtained from the bottom ash and
447 deposits chemical characterization, as part of further research studies.

448 **5. ACKNOWLEDGEMENTS**

449 The authors greatly acknowledge the Spanish Ministry of Science, Innovation and Universities for
450 funding the project “MHWPellet: Mixed pellets based on agricultural crops residues (herbaceous and
451 woody) for their use in the residential sector: optimization of their composition and conversion
452 parameters” (ref. ENE2015-68809-R (MIMECO/FEDER, UE))

453 The authors also would like to thank to Simón Sala, Sebastián Zapata and Roberto Arévalo for their
454 helpful cooperation.

455 **6. REFERENCES**

- 456 [1] Scarlat N., Dallemand J.F., Monforti-Ferrario F., Banja M. Renewable energy policy framework
457 and bioenergy contribution in the European Union – An overview from National Renewable
458 Energy Action Plans and Progress Reports. Renewable and Sustainable Energy Reviews 2015;
459 51: 969-985.
- 460 [2] Scarlat N., Dallemand J.F., Monforti-Ferrario F., Nita V. The role of biomass and bioenergy in a
461 future bioeconomy: Policies and facts. Environmental Development 2015; 15: 3-34.
- 462 [3] Bozell J.J., Black S.K., Myers, M., Cahill, D., Miler W. P. Park, S. Solvent fractionation fo
463 renewable woody feedstocks: Organoslv generation of biorefinery process streams for the
464 production of biobased chemicals. Biomass Bioenergy 2011; 35(10): 4197-208
- 465 [4] Food and Agricultural Organization of the United Nations – FAOSTAT -
466 <http://www.fao.org/faostat/> , accessed in October 2018
- 467 [5] Carvalho L., Wopienka E., Pointner C., Lundgren J., Verma V.K., Haslinger W., Schamidl C.
468 Performance of a pellet boiler fired with agricultural fuels. Applied Energy 2013; 104: 286-296.
- 469 [6] Sippula O., Hytönen K., Tissari J., Raunemaa, T., Jokiniemi, J. Effect of Wood Fuel on the
470 Emissions from a Top-Feed Pellet Stove. Energy & Fuels 2007; 21 (2): 1151-1160.

- 471 [7] Houshfar E., Lovas T., Skreiberg, O. Experimental Investigation on NOX Reduction by Primary
472 Measures in Biomass Combustion: Straw, Peat, Sewage Sludge, Forest Residues and Wood
473 Pellets. *Energies* 2012; 5 (2): 270-290.
- 474 [8] Díaz-Ramírez M., Sebastian F., Royo J., Rezeau A. Influencing factors on NOX emission level
475 during grate conversion of three pelletized energy crops. *Applied Energy* 2014; 115 (0): 360-
476 373.
- 477 [9] Junemann A., Legarreta G. Inhalación de humo de leña: una causa relevante pero poco
478 reconocida de Enfermedad Pulmonar Obstructiva Crónica. *Revista Argentina de Medicina*
479 *Respiratoria* 2007 - Nº 2, 51-57.
- 480 [10] Tian D., Hu Y., Wang Y., Boylan J.W., Zheng M., Russell A.G. Assessment of Biomass Burning
481 Emissions and Their Impacts on Urban and Regional PM2.5: A Georgia Case Study.
482 *Environmental Science Technology* 2009; 43: 299–305
- 483 [11] Christensen K.A., Stenholm M., Livbjerg H. The formation of submicron aerosol particles, HCl
484 and SO2 in straw-fired boilers. *Aerosol Science* 1998; 29 (4): 421-444.
- 485 [12] Saud T., Mandal T.K., Gadi R., Singh D.P., Sharma S.K., Saxena M., Mukherjee A. Emission
486 estimates of particulate matter (PM) and trace gases (SO2, NO and NO2) from biomass fuels
487 used in rural sector of Indo-Gangetic Plain, India. *Atmospheric Environment* 2011; 45 (32):
488 5913-5923.
- 489 [13] Fernández-Llorente M.J., Escalada-Cuadrado R., Murillo-Laplaza J.M., Carrasco-García J.E.
490 Combustion in bubbling fluidised bed with bed material of limestone to reduce the biomass
491 ash agglomeration and sintering. *Fuel* 2006; 85 (14-15): 2081-2092.
- 492 [14] Johansson L.S., Leckner B., Gustavsson L. Cooper D., Tullin C., Potter A. Emission characteristics
493 of modern and old-type residential boilers fired with wood logs and wood pellets.
494 *Atmospheric Environment* 2004; 38 (25), 4183-4195.

- 495 [15] Obernberger I., Biedermann F., widmann W., Riedl R. Concentrations of inorganic elements in
496 biomass fuels and recovery in the different ash fractions. *Biomass and Bioenergy* 1997; 12 (3),
497 211-224.
- 498 [16] Wierzbicka A., Lillieblad L., Pagels J., Strand M., Gudmundsson A., Gharibi A., Swietlicki E.,
499 Sanati M., Bohgard M. Particle emissions from district heating units operating on three
500 commonly used biofuels. *Atmospheric Environment* 2005; 39 (1), 139-150.
- 501 [17] Wiinikka H., Gebart R., Boman C., Boström D., Öhman M. Influence of fuel ash composition on
502 high temperature aerosol formation in fixed bed combustion of woody biomass pellets. *Fuel*
503 2007; 86 (1-2), 181-193.
- 504 [18] Wiinikka H., Gebart R. Experimental investigations of the influence from different operating
505 conditions on the particle emissions from a small-scale pellets combustor. *Biomass and*
506 *Bioenergy* 2004; 27 (6), 645-652.
- 507 [19] Brunner T., Obernberger I., Scharler R. Primary measures for low-emission residential wood
508 combustion-Comparison of old with optimised modern systems. *Proceedings of 17th European*
509 *Biomass Conference and Exhibition, Hamburg, Germany, 2009, 1319-1328.*
- 510 [20] Obernberger I., Brunner T., Bärnthaler G. Chemical properties of solid biofuels--significance
511 and impact. *Biomass and Bioenergy* 2006; 30 (11): 973-982.
- 512 [21] Díaz-Ramírez M., Boman C., Sebastian F., Royo J., Xiong S., Boström D. Ash Characterization
513 and Transformation Behavior of the Fixed-Bed Combustion of Novel Crops: Poplar, Brassica,
514 and Cassava Fuels. *Energy & Fuels* 2012; 26 (6): 3218-3229.
- 515 [22] Díaz-Ramírez, M., Sebastian F., Royo J., Rezeau A. Combustion requirements for conversion of
516 ash-rich novel energy crops in a 250 kWth multifuel grate fired system. *Energy* 2012; 46 (1):
517 636-643.
- 518 [23] Díaz-Ramírez M., Frandsen F.J., Glarborg P., Sebastian F., Royo J. Partitioning of K, Cl, S and P
519 during combustion of poplar and brassica energy crops. *Fuel* 2014; 134 (0): 209-219.

- 520 [24] Boström D, Skoglund N, Grimm A, Boman C, Ohman M, Brostrom M, Backman R. Ash
521 transformation chemistry during combustion of biomass. *Energy & Fuels* 2012; 26: 85–93.
- 522 [25] Becidan M, Houshfar E, Khalil RA, Skreiberg Ø, Løvås T, Sørum L. Optimal Mixtures to Reduce
523 the Formation of Corrosive Compounds during Straw Combustion: A Thermodynamic Analysis.
524 *Energy & Fuels* 2011; 25: 3223-3234
- 525 [26] Khor A, Ryu C, Yang Y-b, Sharifi VN, Swithenbank J. Straw combustion in a fixed bed
526 combustor. *Fuel* 2007; 86: 152-160
- 527 [27] Magdziarz A, Dalai AK, Koziński JA. Chemical composition, character and reactivity of
528 renewable fuel ashes. *Fuel* 2016; 176: 135-145
- 529 [28] Tissari J., Hytönen K., Sippula O., Jokiniemi J The effects of operating conditions on emissions
530 from masonry heaters and sauna stoves. *Biomass and Bioenergy* 2009; 33 (3): 513-520.
- 531 [29] Lamberg H., Sippula O., Tissari J., Jokiniemi J. Effects of Air Staging and Load on Fine-Particle
532 and Gaseous Emissions from a Small-Scale Pellet Boiler. *Energy & Fuels* 2011; 25 (11): 4952-
533 4960.
- 534 [30] Tissari J., Sippula O., Kouki J., Vuorio K., Jokiniemi J. Fine particle and gas emissions from the
535 combustion of agricultural fuels fired in a 20 kW burner. *Energy & Fuels* 2008; 22 (3): 2033-
536 2042.
- 537 [31] Knudsen J.N., Jensen P. A., Dam-Johansen K. Transformation and release to the gas phase of Cl,
538 K, and S during combustion of annual biomass. *Energy & Fuels* 2004; 18 (5): 1385-1399.
- 539 [32] van Lith S.C., Alonso-Ramírez V., Jens P. A., Frandsen F.J., Glarborg P. Release to the gas phase
540 of inorganic elements during wood combustion. Part 1: Development and evaluation of
541 quantification methods. *Energy & Fuels* 2006; 20 (3): 964-978.
- 542 [33] Theis M., Skrifvars B.J., Hupa M., Tran H. Fouling tendency of ash resulting from burning
543 mixtures of biofuels. Part 1: deposition rates. *Fuel*, 2006; 85: 1125–1130.
- 544 [34] Li G., Li S., Xu X., Huang, Q., Yao Q. Dynamic behavior of biomass ash deposition in a 25 kW
545 one-dimensional down-fired combustor. *Energy & Fuels*, 2013; 28: 219-227

- 546 [35] Ryu C., Yang Y.B., Khor A., Yates N. E., Sarifi V.N., Swithenbank J. Effect of fuel properties on
547 biomass combustion: Part I. Experiments – fuel type, equivalence ratio and particle size. *Fuel*,
548 2006; 85 (7-8): 1039-1046
- 549 [36] Houshfar, E., Khalil R.A., Lovas T., Skriberg O. Enhanced NO_x Reduction by Combined Staged
550 Air and Flue Gas Recirculation in Biomass Grate Combustion. *Energy & Fuels*, 2012. 26(5):
551 3003-3011.
- 552 [37] Zhou, H., Jensen A.D., Glarborg P., Kavaliauskas A. Formation and reduction of nitric oxide in
553 fixed-bed combustion of straw. *Fuel*, 2006; 85 (5-6): 705-716
- 554 [38] Andzi-Barhe T., Rogaume T., Richard F., Torero J.L. Numerical characterisation of the
555 mechanisms of NO_x formation during MSW incineration. MCS6. 2009. Ajaccio (France).
- 556 [39] Brunner T., Biedermann F., Kanzian W., Evic N., Obernberger I. Advanced Biomass Fuel
557 Characterization Based on Tests with a Specially Designed Lab-Scale Reactor. *Energy & Fuels*,
558 2013; 27 (10): 5691-5698.
- 559 [40] Wiinikka, H. and Gebart, R. Experimental investigations of the influence from different
560 operating conditions on the particle emissions from a small-scale pellets combustor. *Biomass
561 and Bioenergy*, 2004. 27(6): p. 645-652.
- 562 [41] Zhou, H., Jensen A.D., Glarborg P., Jensen P.A., Kavaliauskas, A. Numerical modeling of straw
563 combustion in a fixed bed. *Fuel*, 2005; 84: 389-403.
- 564 [42] Wiinikka, H. and Gebart, R. Critical Parameters for Particle Emissions in Small-Scale Fixed-Bed
565 Combustion of Wood Pellets. *Energy & Fuels*, 2004. 18(4): p. 897-907.
- 566 [43] Porteiro J., Patiño D., Collazo J., Granada E., Moran J., Miguez J.L. Experimental analysis of the
567 ignition front propagation of several biomass fuels in a fixed-bed combustor. *Fuel*, 2010; 89:
568 26-35
- 569
- 570

- 571 [44] Rezeau A., Royo J., Ribas Cruells J., Masot A., Díaz-Ramírez M., Sala S., Yescas N. Advanced
572 characterization of non-conventional biomass (from emerging markets) in a fixed-bed reactor.
573 Proceedings of 24th European Biomass Conference and Exhibition, Amsterdam, The
574 Netherlands (2016) 801-806
- 575 [45] Díaz-Ramírez M., Maraver D., Rezeau A. Royo J., Sala S., Sebastian F., Sin A. Estimation of the
576 deposition on trigeneration system components fueled by ash rich biomass. Proceedings of
577 20th European Biomass Conference and Exhibition, Milan, Italy (2012) 774-780
- 578 [46] Nunes L.J.R., Matias J.C.O., Catalao J.P.S. Biomass combustion systems: A review on the
579 physical and chemical properties of the ashes. *Renewable and Sustainable Energy Reviews*,
580 2016; 53: 235-242.
- 581 [47] Zeng T., Pollex T., Weller N., Lenz V., Nelles M. Blended biomass pellets as fuel for small scale
582 combustion appliances: Effect of blending on slag formation in the bottom ash and pre-
583 evaluation options. *Fuel* 2018; 212: 108-116
- 584 [48] Öhmana M., Bomana C., Hedmanb H., Nordina A., Boström D. Slagging tendencies of wood
585 pellet ash during combustion in residential pellet burners. *Biomass and Bioenergy* 2004; 27:
586 585–596
- 587 [49] Horttanainen M. V. A., Saastamoinen J. J., Sarkomaa P. J. Operational limits of ignition front
588 propagation against airflow in packed beds of different wood fuels. *Energy & Fuels*, 2002; 16:
589 676–686.
- 590 [50] Regueiro A., Patiño D., Granada E., Porteiro J. Experimental study on the fouling behaviour of
591 an underfeed fixed-bed biomass combustor. *Applied Thermal Engineering*, 2017; 112: 523-533.
- 592 [51] Ryu C., Yang Y.B., Khor A., Yates N.E., Sharifi V.N., Swithenbank J. Effect of fuel properties on
593 biomass combustion: Part I. Experiments—fuel type, equivalence ratio and particle size. *Fuel*,
594 2006; 85: 1039–1046.
- 595 [52] Saastamoinen J. J., Taipale R., Horttanainen M., Sarkomaa P. Propagation of the ignition front
596 in beds of wood particles. *Combustion and Flame*, 2000; 123: 214–226.

- 597 [53] Shin D., Choi S. The combustion of simulated waste particles in a fixed bed. *Combustion and*
598 *Flame*, 2000; 121: 167–180.
- 599 [54] Folgueras M.B., Díaz R. M., Xiberta J., García M. P., Pis J.J. Influence of sewage sludge addition
600 on coal ash fusion temperatures. *Energy&Fuels*, 2005; 19:2562-70
- 601 [55] Madhiyanon T., Sathitruangsak P., Sungworagarn S., Pipatmanomai S., Tia S. A pilot-scale
602 investigation of ash and deposition formation during oil-palm empty-fruit-bunch (EFB)
603 combustion. *Fuel Processing Technology*, 2012; 96:250–264.
- 604 [56] Kleinhans U., Wieland C., Frandsen F.J., Spliethoff H. Ash formation and deposition in coal and
605 biomass fired combustion systems: Progress and challenges in the field of ash particles sticking
606 and rebound behavior. *Progress in Energy and Combustion Science*, 2018; 68:68-168
- 607 [57] Niu Y., Tan H., Hui S. Ash-related issues during biomass combustion: Alkali-induced slagging,
608 silicate melt-induced slagging (ash fusion), agglomeration, corrosion, ash utilization, and
609 related countermeasures. *Progress in Energy and Combustion Science*, 2016; 52: 1-61
- 610 [58] Baxter L.L., Miles T.R., Jenkins B.M., Milne T., Dayton D., Bryers R.W., Oden L.L. The behavior of
611 inorganic material in biomass-fired power boilers: field and laboratory experiences. *Fuel*
612 *Processing Technology*, 1998; 54: 47–78.
- 613 [59] Teixeira P., Lopes H., Gulyurtlu I., Lapa N., Abelha P. Evaluation of slagging and fouling
614 tendency during biomass co-firing with coal in a fluidized bed. *Biomass and Bioenergy*, 2012;
615 39: 192–203.
- 616 [60] Thy P, Jenkins BM, Grundvig S, Shiraki R, Leshner CE. High temperature elemental losses and
617 mineralogical changes in common biomass ashes. *Fuel*, 2006; 85:783–95.
- 618 [61] Theis M., Skrifvars B.-J., Zevenhoven M., Hupa M., Tran H. Fouling tendency of ash resulting
619 from burning mixtures of biofuels. Part 2: deposit chemistry. *Fuel*, 2006; 85: 1992–2001.
- 620 [62] Skrifvars B-J, Laure´n T, Hupa M, Korbee R, Ljung P. Ash behavior in a pulverized wood fired
621 boiler – a case study. *Fuel* 2004; 83:1371–9.

- 622 [63] Robinson AL, Junker H, Baxter LL. Pilot-scale investigation of the influence of coal-biomass
623 cofiring on ash deposition. *Energy Fuels* 2002; 16:343–55.
- 624 [64] van Lith S. C., Jensen P. A., Frandsen F. J., Glarborg P. Release to the Gas Phase of Inorganic
625 Elements during Wood Combustion. Part 2: Influence of Fuel Composition. *Energy & Fuels*,
626 2008; 22: 1598–1609
- 627 [65] Johansen J. M., Aho M., Paakinen K., Taipale R., Egsgaard H., Jakobsen J. G., Frandsen F. J.,
628 Glarborg P. Release of K, Cl, and S during combustion and co-combustion with wood of high-
629 chlorine biomass in bench and pilot scale fuel beds. *Proceedings of the Combustion Institute*,
630 2013; 34: 2363–2372.